Доклади на Българската академия на науките
Comptes rendus de l'Académie bulgare des Sciences

Tome 75, No 7, 2022

GEOLOGY
Geochemistry

REE AND TRACE ELEMENTS DISTRIBUTION IN THE DEEP-SEA SEDIMENTS FROM THE INTEROCEANMETAL (IOM) POLYMETALLIC NODULE EXPLORATION AREA IN THE CLARION-CLIPPERTON FRACTURES ZONE, NE PACIFIC

Atanas Hikov, Zlatka Milakovska, Valcana Stoyanova*, Elitsa Stefanova, Tomasz Abramowski*,, Silvia Chavdarova, Milen Stavrev**

Received on February 1, 2022
Presented by I. Zagorchev, Member of BAS, on March 29, 2022

Abstract

Geochemical features of the deep-sea sediments from a high polymetallic nodule area in the eastern part of the Clarion-Clipperton Fractures Zone (CCZ), NE Pacific were studied. Box-corer samples from six stations in individual depth layers 0–3, 3–5, 5–10, 10–20 cm were collected from 4300–4500 m depth. The deep-sea sediments were classified as clayey-siliceous oozes according to the mineral and grain-size analyses. The chemical composition of the studied samples is compatible with that of pelagic sediments. Manganese content varies from 0.16% to 0.70% being the highest in the geochemically active layer (top 7–12 cm) and decreases with depth. The Mn/Fe ratio, Ba, Co, Ni and Cu have the highest values in the first (0–3) and second (3–5) layers and decrease with depth. ΣREE range is 195.84–357.79 ppm showing low variation between the layers. PAAS-normalized REE patterns show significant enrichment of MREE and HREE with strong negative Ce anomaly and weak positive Eu and Y anomalies. The geochemical characteristics of the studied sediments infer polygenic origin. The redox sensitive oxides and barite presense, Eh values and negative Ce anomaly, indicate oxidizing environment of sediment formation.

Key words: deep-sea sediments, polymetallic nodules, geochemistry, REE, Interoceanmetal, Clarion-Clipperton Fractures zone

The study was supported by Bulgarian National Science Fund grant KP-06-N34/6.
DOI:10.7546/CRABS.2022.07.10

Introduction. The growth of world economy and new emerging technologies resulted in growing demand for rare and trace elements defined as critical raw materials for the European Union [1]. One of the most promising new raw materials are deep-sea metalliferous sediments and manganese-iron (Mn–Fe) polymetallic nodules and crusts formed in modern environments at the ocean floor (> 4000 m depth). The interest towards nodules rose after research studies determined them as a potential source for high-tech elements from the rare earth group (REE), especially heavy REEs and yttrium (Y) and scandium (Sc) [2–4]. The Fe–Mn Nodule bearing Clarion–Clipperton Zone (CCZ) in the NE Pacific and the Fe–Mn prime crust zone (PCZ) in the central Pacific are the areas of greatest economic interest for nodules, crusts and sediments [2,5]. Recent research indicated that deposits of polymetallic nodules have the potential to be economically feasible for exploitation in the presence of favourable metal prices, as well as with the technological improvement of mining and processing systems [6].

The aim of the research is to study the natural spatial and vertical geochemical variabilities of the deep-sea sediments from a high polymetallic nodule area in the eastern part of the CCZ, NE Pacific. The samples were collected from 4300–4500-m depth during the 2019 Interoceanmetal (IOM) cruise. The survey of the polymetallic nodule resources requires knowledge on both sediments and nodules in order to estimate their value and the anticipated environmental impact during the potential mining operations.

Geological setting and sampling. The area examined, represents the most perspective for nodule exploitation part of the IOM licence area designated as the H22_NE exploitable block, covers 630 km^2 of the seafloor, in the eastern part of the Clarion-Clipperton fractures Zone, NE Pacific between 11°06′–11°26′N latitude and 119°25′–119°42′W longitude at depth varying from 4300 to 4500 m (Fig. 1). The stations explored were distributed among various geomorphological types, represented mostly by undulating hilly plains, intersected by longitudinal ridges oriented in the meridional direction, and a sub-parallel volcanic massif. All stations sampled are located below the critical carbonate compensation depth. The sedimentary cover within the IOM exploration area is about 100 m thick. The sediment profile is topped by slightly siliceous silty clay and siliceous silty clay. Sediments of this layer contain 3.04–28.6% of amorphous silica and are characterized by reduced bulk density and increased moisture content. The sedimentation rate in the IOM site ranges between 0.2 and 1.15 cm/kyr [7,8].

Box-corer samples from six stations of individual depth layers 0–3, 3–5, 5–10, 10–20 cm were collected during the IOM'2019 expedition. Data on board processing of sampled stations showed that wet nodule abundance parameter ranges from 10.3 to 19.9 kg/m^2, averaging 13.5 kg/m^2; whereas the nodule coverage calculated using spot photographs of the seabed varies from 18 to 50% with an average of 40%.

Sedimentological characteristics. The sediment composition at all stations is dominated by light brown siliceous silty clays with irregular dark patches

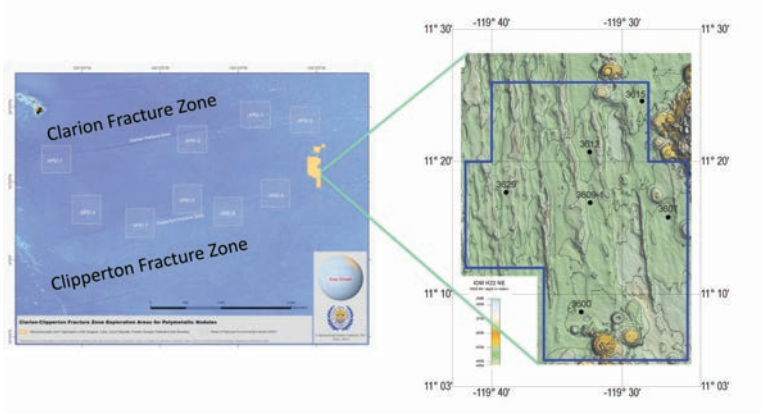

Fig. 1. Geomorphological map of the seafloor and location of sampling area in the IOM exploration site in the eastern part of the Clarion-Clipperton fractures zone (CCZ), NE Pacific

along the entire core down to 45 cm in depth (Fig. 2). The top 7–12 cm layer comprises a semiliquid, predominantly dark brown-coloured, siliceous silty clay, denoted as geochemically active layer (GAL), the medium for polymetallic nodule formation. The redox potential (Eh) value of the GAL ranges from +462 mV to +545 mV (average +494 mV) and indicates a tendency to decrease with depth. Maximum redox potential values were obtained for slightly siliceous silty clay at station no. 3615 at the depth of 30 cm – +547 mV. The sediments at this sta-

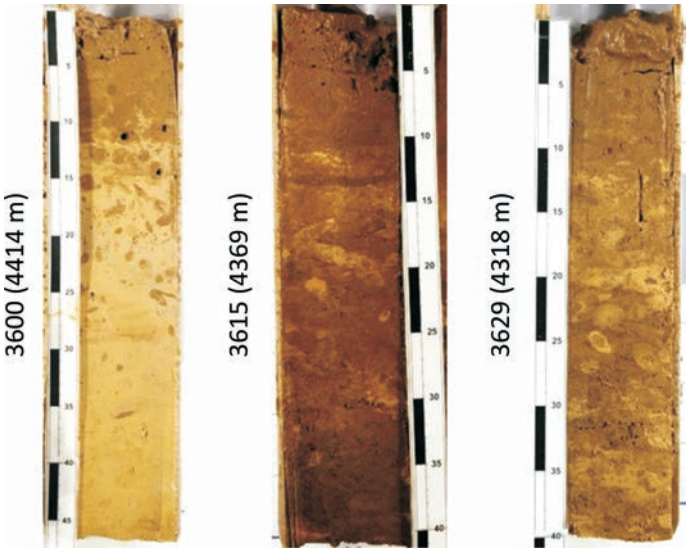

Fig. 2. Sediment core sections from sampling stations 3600, 3615 and 3629

tion were characterized by dark colour and abundant radiolarian skeletons, sponge spicules, micronodules, and clay aggregates. The active reaction (pH) of the environment is mostly neutral for all sediments examined, changing weakly from 7.01 to 7.52, averaging 7.36 [9].

The authors' preliminary results on bulk samples indicated that the sediments are composed of fine silts. They are predominantly poorly sorted with bimodal particle size distribution. The silt (50–84%) and sandy (9–31%) fractions show opposite trends, whereas the clayey fraction increases with depth. The mineral composition according to the XRD data is uniform in quality and quantity. An amorphous phase (84–88%) predominates, representing biogenic opal, authigenic Fe–Mn (hydr)oxides and clay minerals. This phase composition defines the sediments as clayey siliceous ooze. The crystalline phases illite, kaolinite, chlorite, quartz, andesine represent a detrital component, while halite, cristobalite and barite are of authigenic origin. Illite, illite/smectite, chlorite/vermiculite and kaolinite, and quartz admixture were detected in all fractions < 2 μm [9].

Methods. Box corer (with a 0.25 m^2 sampling area) was used to yield relatively undisturbed bottom samples up to 50 cm in the sediment depth. After recovery of the box corer onboard, the near-bottom water overlying the sample was siphoned out and photos were taken to document the sediment surface as well as the natural distribution of nodules and associated benthic fauna. The nodules from the sediment surface were then collected and samples of sediment into four depth layers: 0–3, 3–5, 5–10, 10–20 cm were taken. Major element composition was determined by ICP-OES at AQUATERATEST LTD, Sofia. Trace elements were measured on fused pellets by LA-ICP-MS at the Geological Institute of Bulgarian Academy of Sciences, using laser ablation system New Wave UP193FX coupled to a PerkinElmer ELAN DRC-e ICP-MS. The laser beam diameter was 100 μm and laser pulse frequency of 10 Hz was used. The NIST 610 was used for external standard and SiO_2, determined by ICP-OES as internal standard. Data reduction was done using SILLS ver. 1.1.0 software.

Results. The chemical composition of the sediment samples is similar with some small differences according to the station and depth interval (Table 1). Concentrations of Si (23.63–26.33%), Al (6.20–7.38%) and Ti (0.32–0.38%) show low variations between the layers and slightly increase with depth, especially Al and Ti in the fourth layer (10–20 cm). Sodium (3.44–4.38%) has higher content for the first (0–3 cm) and second (3–5 cm) layers compared to the other two layers while Mg (1.80–2.04%) and K (1.99–2.45%) weakly increase in the fourth layer. Calcium (0.70–0.94%), P (0.07–0.16%) and S (0.53–0.84%) do not show any significant variations between layers.

Iron content ranges from 4.10% to 4.99% (average 4.60%) and slightly increases with depth (Fig. 3a). Manganese varies from 0.16% to 0.70% (average 0.49%) being the highest for the first layer (0–3 cm) and the geochemically active layer (the top 7–12 cm) and decreasing with depth (Fig. 3a). The Mn/Fe ratio

Table 1

Mean values of major and trace elements in individual depth layers 0–3, 3–5, 5–10, 10–20 cm from six stations

layers	Si	Al	Ti	Ca	Mg	Na	K	P	S	Fe	Mn	Ba	V	Rb	Sr	Zr	Nb	Ga	Ge
cm	wt.%	wt.%	wt.%	wt.%	wt.%	wt.%	wt.%	wt.%	wt.%	wt.%	wt.%	wt.%	ppm	ppm	ppm	ppm	ppm	ppm	ppm
0–3	24.71	6.45	0.33	0.85	1.91	3.97	2.11	0.13	0.60	4.40	0.60	0.96	121.9	87.45	385.6	151.3	9.83	22.9	3.10
3–5	24.68	6.56	0.34	0.86	1.92	3.93	2.14	0.12	0.67	4.44	0.58	0.95	120.1	86.67	379.1	149.8	9.77	22.0	3.38
5–10	25.31	6.65	0.34	0.84	1.91	3.61	2.12	0.12	0.65	4.51	0.51	0.98	119.8	94.63	390.3	161.4	10.58	21.4	2.40
10–20	25.14	6.94	0.67	0.83	1.96	3.60	2.25	0.11	0.62	4.66	0.28	0.86	119.4	91.36	348.5	153.1	10.22	22.0	3.05
layers	Cr	Co	Ni	Cu	Zn	Mo	Ag	Sn	W	Pb	As	Sb	Bi	Cs	Hf	Ta	Sc	Th	U
cm	ppm	ppm	ppm	ppm	ppm	ppm	ppm	ppm	ppm	ppm	ppm	ppm	ppm	ppm	ppm	ppm	ppm	ppm	ppm
0–3	88.36	72.44	190.0	403.9	122.4	7.86	2.86	2.42	6.23	22.19	15.19	1.86	0.81	6.75	3.80	0.72	26.85	10.02	1.65
3–5	94.97	67.95	173.6	392.3	119.7	8.24	2.72	2.51	5.69	21.56	14.91	1.62	0.64	6.70	3.70	0.70	27.16	9.72	1.60
5–10	104.9	63.59	159.1	365.8	116.9	7.57	2.47	2.52	5.82	22.35	14.19	1.56	0.56	7.44	3.97	0.65	29.76	10.93	1.82
10–20	96.98	52.35	99.34	310.8	110.4	5.66	3.22	2.78	4.99	23.26	13.67	1.34	0.73	7.29	3.73	0.64	26.96	10.19	1.61
layers	Y	La	Ce	Pr	Nd	Sm	Eu	Gd	Tb	Dy	Ho	Er	Tm	Yb	Lu	ΣREE	ΣREY	ΣHREE	Mn/Fe
cm	ppm	ppm	ppm	ppm	ppm	ppm	ppm	ppm	ppm	ppm	ppm	ppm	ppm	ppm	ppm	ppm	ppm	ppm	
0–3	68.56	45.09	72.11	12.80	52.49	12.98	3.34	12.97	2.03	12.10	2.39	6.69	0.97	6.42	0.95	243.3	311.9	47.85	0.14
3–5	68.56	44.56	71.12	12.69	51.75	12.94	3.19	13.11	1.97	11.73	2.39	6.66	0.92	6.27	0.95	240.2	308.8	47.19	0.13
5–10	72.85	47.38	76.71	13.54	55.70	13.42	3.51	13.62	2.14	12.61	2.52	7.02	1.02	6.82	1.05	257.1	329.9	50.30	0.11
10–20	68.80	44.97	72.86	12.81	52.37	12.30	3.19	12.92	1.95	11.85	2.38	6.76	0.97	6.25	0.96	242.5	311.3	47.23	0.06

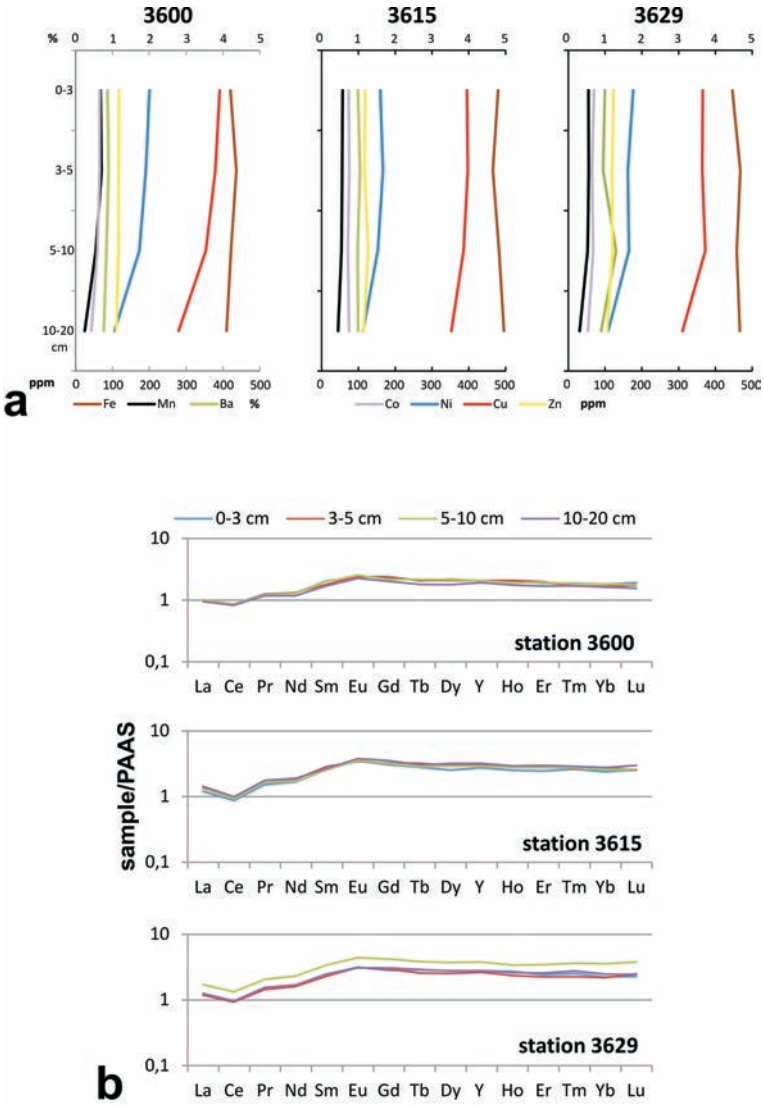

Fig. 3. Geochemical variations in sample stations 3600, 3615 and 3629: a) Vertical distribution of selected metals in individual depth layers 0–3, 3–5, 5–10, 10–20 cm; b) PAAS-normalized REE patterns of four depth layers

varies from 0.03 to 0.16 (average 0.11) being the highest for the GAL and decreases with depth (Table 1). The highest Mn concentrations were recorded for stations 3600 and 3615. The elements defined as characteristic for the metalliferous sediments are as follows (ppm): Cr – 71–130 (av. 96.32), Co – 41.6–86.8 (64.08), Ni – 80.24–216.80 (155.52), Cu – 280–429.5 (368.19), Zn – 105.5–132 (117.34). Cobalt, Ni and Cu have the highest concentrations in the first (0–3 cm) and second (3–5

cm) layers and decrease with depth while Cr and Zn do not show such trend (Fig. 3a). Cobalt and Cu are higher in station 3615 compared to the other stations while the highest Ni was measured for station 3600.

Barium varies from 0.77% to 1.04% (average 0.94%) showing small variations between layers being the highest for the GAL and decreases with depth (Fig. 3a). The northern stations (3629 and 3615) have the highest Ba and P content. Yttrium values vary between 51.61 and 101.69 ppm (average 69.69 ppm).

Rare-earth elements provoke a special interest to deep-sea sediments. The ΣREE in the studied samples varies from 195.84 to 357.79 ppm (average 245.79 ppm). The ΣHREE ranges from 34.17 to 71.03 ppm (average 48.14 ppm) and the ΣREY – between 247.44 and 457.91 ppm (average 315.48 ppm). The northern stations (3629 and 3615) have the highest REE and Y content without any significant variations of these elements between layers, being higher in the third (5–10 cm) layer. Chondrite-normalized REE patterns are similar with negative Ce ($Ce/Ce^* = 0.73$) and Eu ($Eu/Eu^* = 0.77$) anomalies. Both NASC and PAAS-normalized REE patterns show close values for LREE and significant enrichment of MREE and HREE (Fig. 3b). All samples show strong negative Ce ($Ce/Ce^* = 0.70$) anomaly, positive Eu ($Eu/Eu^* = 1.19$) and weak positive Y ($Y/Y^* = 1.03$) anomalies.

Aluminium has strong (0.7–1) positive correlation with Fe, Ti, K and Mg, moderate (0.5–0.69) correlation with Ca and weak (0.3–0.49) – with P, Ga, Y, Zr, Nb and most of REE. Iron shows strong positive correlation with Ti, K, Mg, Ca and moderate to weak correlation with P, Ga, Y, REE. There is a negative correlation between all these elements and Mn. On the other hand, Mn has a strong positive correlation with Co, Ni and Cu, moderate with Zn, Mo, W, weak correlation with Na, Sr, Sb, Ba and negative with Pb. Cobalt, Ni, Cu, Zn, Mo and W have strong- to moderate positive correlation with each other and weak correlation with Ba, V and Ga. Strong- to moderate positive correlation is recorded between Sc, Rb, Sr, Y, Zr, Nb, Cs, Ba, most of REE, Th and U and between them and P and Ca.

Discussion and conclusions. The chemical composition of the sediments studied is comparable to this of pelagic sediments [10]. The sediments have elevated concentrations for Na, S, Sr, Ba, Sc, Ge, Cu, Ag, Sb, W, Y, MREE and HREE, lower concentrations for Al, Si, Fe, Mn, P, V, Zr, Nb, Ta, Pb, As, Mo and Ce, and approximately the same concentrations of Ti, Mg, Ca, K, Ga, Cr, Co, Ni, Zn, Pb, Bi, Sn, Cs, Hf, Th, U, La and Nd. The concentrations of most of the elements are similar to those published for the other parts of CCZ [11], as well as to the samples from the first horizon A (0–5 cm) from the neighbour H11 block of IOM [12].

The correlation between major and trace elements reflects the mineral composition of the studied sediments. The first group of elements includes Al, Fe, Ti, K, Mg, partly Ca and represents a detrital (illite, kaolinite, chlorite) and volcanic

(andesine) mineral composition and quartz. Silicon is only partly associated with this group due to additional independent input of siliceous radiolarian skeletons, diatom frustules and spongian spicules [9–11]. The second group includes Mn, Co, Ni, Cu, Zn, Mo, W. These elements are preferentially incorporated into MnO_2 phases [5,13]. The polymetallic nodules were removed from the studied sediments but they contain a certain amount of micronodules [9], which contain the elements listed. The third group of elements (Sc, Rb, Sr, Y, Zr, Nb, Cs, Ba, REE, Th, U as well as P and Ca) comprises authigenic mineral phases – mostly barite and apatite [10–12].

The carriers of REY in deep-sea sediments include aluminosilicate, Fe–Mn (oxy)hydroxides, and phosphate components [5,14–16]. The ΣREY of the phosphate component is 1–2 orders of magnitude higher than those of the other two carriers [14]. The Fe–REE positive correlation shows that a part of the REE may be incorporated into Fe (oxy)hydroxide phases [5,15]. On the other hand, the clay minerals are likely more significant REE host phases than Fe–Mn (oxy)hydroxides [16,17].

The studied deep-sea sediments from the eastern part of the CCZ, NE Pacific have high Al/(Al + Fe + Mn) ratio (0.57) and could be considered non-metalliferous [18], although they host significant amount of Fe–Mn nodules. As a part of the chain deep-sea water–sediment–nodules we have to characterize the sediment features. The nodules occur predominantly on the surface of sediment-covered abyssal plains partly or completely buried in the sediment [5] mostly in the geochemically active layer (the top 7–12 cm). In this environment, they interact with oceanic water (hydrogenetic precipitation), or with the pore water of host sediments (diagenetic precipitation) [5,13]. The elevated content of some elements (Mn, Co, Cu, Ba, P, Y, REE) in the northern station 3615 and partly in station 3600 suggests some input from the adjacent volcanics [12]. The Ce/La ratio 1.44–1.82 (mean 1.61) indicates hydrothermal processes (< 2) input [12]. Most probably the studied sediments have mixed polygenic origin.

The ΣREE values lower than for the metalliferous deep-sea mud [2] define the sediments studied as non-metalliferous irrespectively of the elevated REE content compared to the pelagic sediments [10] and close to the sediments from other parts of CCZ [11]. On the other hand, the polymetallic nodules from the same stations as well as from the whole CCZ contain ΣREE 2–3 times higher than the sediments in addition to a significant MREE and HREE enrichment [11,19,20], so REE could be considered a significant by-product in the future nodules exploitation.

PAAS-normalized REE patterns show strong negative Ce anomaly and suggest oxidizing environment of formation [15]. Increase of the bone debris content in the pelagic clay as a result of low sedimentation rates leads to depletion in Ce and LREE, because the bone debris accumulates considerable amounts of REE dissolved in the oceanic water probably without any noticeable fractionation [15]. The phosphate component is mainly composed of P, Ca, Sr, REY, Sc, U, and

Th, and its chemical composition is considered relatively stable [14]. The phosphate component has a negative Ce anomaly and positive Y anomaly. After the early diagenetic processes (biogeochemistry, adsorption, desorption, transformation, and migration), the REY enrichment in the phosphate component is completed near the seawater/sediment interface. The REY enrichment is a result of several factors, including low sedimentation rate, high REY of the bottom seawater, a non-carbonate depositional environment, oxidation conditions, and certain bottom current conditions [14].

The geochemical characteristics of the studied sediments infer polygenic origin. The negative Ce anomaly is in agreement with Eh values, redox sensitive oxides and barite presence, all reflecting an oxidizing environment of formation [9]. These conditions are a medium for polymetallic nodule formation and high nodule abundance was delineated where Eh was high enough ($> +500$ mV) [7].

REFERENCES

[1] COM (2020) 474, Critical Raw Materials Resilience: Charting a Path towards greater Security and Sustainability, European Commission, 23 pp.

[2] Kato Y., F. Fujinaga, K. Nakamura, Y. Takaya, K. Kitamura et al. (2011) Deep-sea mud in the Pacific Ocean as a potential resource for rare-earth elements, Nature Geoscience, **4**, 535–539.

[3] Yasukawa K., J. Ohta, K. Mimuraa, E. Tanaka, Y. Takaya et al. (2018) A new and prospective resource for scandium: Evidence from the geochemistry of deep-sea sediment in the western North Pacific Ocean, Ore geol. Rev., **120**, 260–267.

[4] Pak S. J., I. Seo, K. Y. Lee, K. Hyeong (2019) Rare Earth Elements and Other Critical Metals in Deep Seabed Mineral Deposits: Composition and Implications for Resource Potential, Minerals, **9**, 1–19.

[5] Hein J., K. Mitzell, A. Koschinsky, T. Conrad (2013) Deep-ocean mineral deposits as a source of critical metals for high- and green-technology applications: Comparison with land-based resources, Ore Geol. Rev., **51**, 1–14.

[6] Abramowski T., M. Urbanek, P. Baláž (2021) Economic Assessment of Polymetallic Nodules Mining Project with Updates to Present Market Conditions, Minerals, **11**, 311, 1–21.

[7] Baláž P. (2021) Results of the first phase of the deep-sea polymetallic nodules geological survey in the Interoceanmetal Joint Organization licence area (2001–2016), Mineralia Slovaca, **53**, 3–36.

[8] Skowronek A., L. Maciag, D. Zawadzki, A. Strzelecka, P. Baláž et al. (2021) Chemostratigraphic and Textural Indicators of Nucleation and Growth of Polymetallic Nodules from the Clarion-Clipperton Fracture Zone (IOM Claim Area), Minerals, **11**, 868, 1–38.

[9] Milakovska Z., V. Stoyanova, A. Hikov, T. Abramowski, E. Stefanova et al. (2021) Depositional setting of the deep-sea sediments from an area of high nodule occurrence in the Clarion-Clipperton Fractures Zone, NE Pacific, Goldschmidt 2021 Abstract, https://doi.org/10.7185/gold2021.5983

[10] Li Y-H., J. E. Schoonmaker (2014) Chemical Composition and Mineralogy of Marine Sediments, Treatise on Geochemistry, 2nd Edition, **9**(1), 1–35.
[11] Menendez A., R. James, A. Lichtschlag, D. Connelly, K. Peel (2019) Controls on the chemical composition of ferromanganese nodules in the Clarion-Clipperton Fracture Zone, eastern equatorial Pacific, Marine Geology, **409**, 1–14.
[12] Zawadzki D., J. Maciag, T. Abramowski, K. McCartney (2020) Fractionation Trends and Variability of Rare Earth Elements and Selected Critical Metals in Pelagic Sediment from Abyssal Basin of NE Pacific (Clarion-Clipperton Fracture Zone), Minerals, **10**, 320, 1–38.
[13] Halbach P., C. Scherhag, U. Hebisch, V. Marchig (1981) Geochemical and mineralogical control of different genetic types of deep-sea nodules from the Pacific Ocean, Mineralium Deposita, **16**, 59–84.
[14] Ren J., Y. Liu, F. Wang, G. He, X. Deng et al. (2021) Mechanism and Influencing Factors of REY Enrichment in Deep-Sea Sediments, Minerals, **11**, 196, 1–16.
[15] Dubinin A. (2004) Geochemistry of Rare Earth Elements in the ocean, Lithology and mineral resources, **39**, 289–307.
[16] Abbott A., S. Löhr, M. Trethewy (2019) Are Clay Minerals the Primary Control on the Oceanic Rare Earth Element Budget?, Front. Mar. Sci., **6**, 504.
[17] Sa R., X. Sun, G. He, L. Xu, Q. Pan et al. (2018) Enrichment of rare earth elements in siliceous sediments under slow deposition: A case study of the central north Pacific, Ore Geol. Rev., **94**, 12–23.
[18] Bostrom K. (1973) The origin and fate of ferromanganese active ridge sediments, Stockholm contributions to geology, **27**, 149–243.
[19] Dimitrova D., Z. Milakovska, I. Peytcheva, E. Stefanova, V. Stoyanova et al. (2014) Trace element and REY composition of polymetallic nodules from the Eastern Clarion–Clipperton Zone determined by in-situ LA-ICP-MC analyses, C. R. Acad. Bulg. Sci., **67**(2), 269–276.
[20] Stoyanova V., A. Hikov, E. Stefanova, Z. Milakovska, T. Abramowski et al. (2021) Deep-sea polymetallic nodules as opportunity for future supply with critical raw materials, Rev. Bulg. Geol. Soc., **82**(3), 153–155.

Geological Institute
Bulgarian Academy of Sciences
Akad. G. Bonchev St, Bl. 24
1113 Sofia, Bulgaria
e-mail: ahikov@geology.bas.bg
zlatkam@geology.bas.bg
stefanova_e@geology.bas.bg
silvia.chavdarova@gmail.com
milen_stavrev07@abv.bg

[*] *Interoceanmetal Joint Organization*
9 Cyryla I Metodego St
71541 Szczecin, Poland
e-mail: v.stoyanova@iom.gov.pl
t.abramowski@iom.gov.pl

[**] *Maritime University of Szczecin*
71541 Szczecin, Poland
e-mail: t.abramowski@am.szczecin.pl